



# Quantitative Monte Carlo-based brain dopamine transporter SPECT imaging

Tuija Kangasmaa<sup>1</sup> · Eero Hippeläinen<sup>2</sup> · Chris Constable<sup>3</sup> · Sampsa Turunen<sup>2</sup> · Antti Sohlberg<sup>3,4</sup>

Received: 28 May 2020 / Accepted: 16 September 2020 / Published online: 25 September 2020  
© The Japanese Society of Nuclear Medicine 2020

## Abstract

**Objective** Brain dopamine transporter imaging with I-123-labeled radioligands is technically demanding due to the small size of the imaging target relative to the spatial resolution of most SPECT systems. In addition, I-123 has high-energy peaks which can penetrate or scatter in the collimator and be detected in the imaging energy window. The aim of this study was to implement Monte Carlo (MC)-based full collimator–detector response (CDR) compensation algorithm for I-123 into a third-party commercial SPECT reconstruction software package and to evaluate its effect on the quantitative accuracy of dopaminergic-image analysis compared to a method where only the geometric component of the CDR is compensated.

**Methods** In this work, we utilized a full Monte Carlo collimator–detector model and incorporated it into an iterative SPECT reconstruction algorithm. The full Monte Carlo model reconstruction was compared to standard reconstruction using an anthropomorphic striatal phantom filled with different I-123 striatal/cortex uptake ratios and with clinical I-123 Ioflupane DaTScan studies.

**Results** Reconstruction with the full model yielded higher (13–25%) striatal uptake ratios than the conventional reconstruction, but the uptake ratios were still much lower than the true ratios due to partial volume effect. Visually, images reconstructed with the full Monte Carlo model had better contrast and resolution than the conventional images, with both phantom and patient studies.

**Conclusions** Reconstruction with full Monte Carlo collimator–detector model yields higher quantitative accuracy than conventional reconstruction. Additional work to reduce the partial volume effect related errors would improve the accuracy further.

**Keywords** SPECT · I-123 · Monte Carlo · Full collimator–detector model · Phantom

## Introduction

Parkinson disease is a very common neurodegenerative disorder with symptoms attributed mainly to dopamine deficit [1, 2]. Iodine-123-labeled pharmaceuticals are used in clinical SPECT brain imaging of the dopaminergic system to diagnose Parkinsonian syndromes and they might be useful to monitor disease progression and effects of therapy [3–6]. For objective and more accurate evaluation, quantitative analysis is recommended [4, 5]. For brain SPECT imaging striatal/cortex volume of interest (VOI) count ratios are widely used for quantitative analysis. However, quantitative analysis is sensitive to a number of factors including photon attenuation and scatter, collimator–detector response (CDR), partial volume effect (PVE), dead-time, radioactive decay and patient/organ motion [6–8].

✉ Tuija Kangasmaa  
tuija.kangasmaa@vshp.fi

<sup>1</sup> Department of Clinical Physiology and Nuclear Medicine, Vaasa Central Hospital, Hietalahdenkatu 2-4, 65130 Vaasa, Finland

<sup>2</sup> Clinical Physiology and Nuclear Medicine, HUS Medical Imaging Center, University of Helsinki and Helsinki University Hospital, Haartmaninkatu 4, 00029 Helsinki, Finland

<sup>3</sup> HERMES Medical Solutions, Strandbergsgatan 16, 11251 Stockholm, Sweden

<sup>4</sup> Laboratory of Clinical Physiology and Nuclear Medicine, Päijät-Häme Central Hospital, Keskussairaalankatu 7, 15850 Lahti, Finland

The most abundant gamma emission of I-123 (159 keV) is well-suited to SPECT imaging with low-energy high-resolution (LEHR) collimators, but about 3% of emitted photons have higher energies than 159 keV [6]. The thin septa of LEHR collimators allow a significant number of these photons to penetrate through and scatter within the collimator and some of these photons are detected in the 159 keV acquisition energy window.

Compensation for the collimator detector response (CDR) during image reconstruction is essential for quantitative imaging [7, 9]. In addition, correcting for the CDR decreases the artifacts resulting from PVE [9]. CDR consists of geometric, septal penetration and collimator scatter components, and is considered one of the most important degrading factors for quantitative SPECT accuracy [10]. While the geometric component can be modeled analytically, the two other components are more challenging to model. Many commercial reconstruction software packages model only the geometric component, and while this works relatively well for low-energy emitting isotopes (e.g., Tc-99 m), it is not well-suited for high-energy emitting isotopes [7]. There have also been approaches to model the full CDR with Monte Carlo (MC)-based algorithms [6, 8, 10, 11]. While they can provide more accurate results, they are not only challenging to implement, but also computationally demanding.

The aim of this study was to implement MC-based full CDR compensation algorithm for I-123 into a third-party commercial SPECT reconstruction software package and to evaluate its effect on the quantitative accuracy of dopaminergic-image analysis compared to a method where only the geometric component of the CDR is compensated.

## Material and methods

### Reconstruction methods

The reconstruction algorithms were based on the ordered subsets expectation maximization (OS-EM) algorithm [12, 13] with rotation-based [14] projectors. Attenuation was modeled using a CT-based attenuation map, which was generated by converting Hounsfield units in the CT images into linear attenuation coefficients by bilinear scaling. The geometric component of the CDR assumed Gaussian point-spread functions (PSFs) and considered only the primary, 159 keV, peak. Patient scatter was compensated using the conventional convolution-based forced detection MC model [15]. Henceforth, this algorithm will be called Gauss MC.

I-123 also emits photons with energies higher than 159 keV. To handle these high-energy emissions, the conventional convolution-based forced detection model was updated to support the higher energies. In the conventional

convolution-based forced detection model, the scattering path of a photon with a starting energy of 159 keV is followed using the MC method. A copy of the simulated photon is forced to scatter towards the detector at each interaction site and a 3D sub-projection map is updated by the photon's weight [15]. The sub-projection map's energy window corresponds to the acquisition energy window. After all photons have been simulated, the 3D sub-projection map is forward projected assuming Gaussian CDR to form scatter projections. In order to model the higher energy photons the conventional convolution-based forced detection model was modified to use five sub-projection maps with the following energies: acquisition lower energy level-acquisition higher energy level, acquisition higher energy level-300, 300–400, 400–500 and 500–550 keV. These five energy windows allowed the tracking of photons with starting energies higher than 159 keV. The Gaussian PSFs also had to be replaced with MC pre-simulated PSFs generated using the simulator presented in [16]. Distance-dependent PSFs were calculated for each of the five sub-projection map energy windows by simulating point sources emitting photons corresponding to the center energy of the sub-projection map that were detected in the acquisition energy window. The pre-simulated PSFs take collimator scatter and penetration into account. We call this second algorithm Full MC. Both algorithms are presented in more detail in [17] and they were implemented as part of the HERMES HybridRecon (Hermes Medical Solutions, Stockholm, Sweden) reconstruction package.

For both algorithms, images were reconstructed with 10 iterations, 16 subsets and 0.8 cm FWHM Gaussian 3D post-filter according to our clinical practice.

### Phantom acquisition and processing

Striatal uptake ratios (SURs) were used to compare the two algorithms. SUR is defined as  $(Cs-Cb)/Cb$ , where Cs is the striatal activity or count concentration and Cb the background activity or count concentration.

The anthropomorphic striatal phantom (Radiological Support Services Inc. Long Beach, CA, USA) was filled several times with I-123 to give SURs of 9.6, 4.6, 2.8, 2.3, 1.8 and 1.3 which is a typical range seen in clinical practice. The SURs were varied by changing the background activity (from 223 Bq/ml to 1029 Bq/ml), while the activity of striatum was constant (2367 Bq/ml). Both the caudate and putamen compartment were filled with the same activity concentration. The true ratios ( $SUR_{true}$ ) were determined by taking aliquots from each filling solution which were then measured in a well counter (Hidex Oy, Turku, Finland).

The I-123 phantom was scanned with a Siemens Symbia T (Siemens Healthineers, Erlangen, Germany) gamma camera with LEHR collimators, 15% energy window centered

on 159 keV,  $128 \times 128$  matrix, 3.3 mm pixel size, 120 angles and 30 s per projection. The CT parameters in all studies were 130 kV, 30 mAs and 1.5 pitch. CT images were reconstructed into  $512 \times 512$  matrix, with 0.98 mm pixel size and 3.0 mm slice thickness.

Reconstructed SPECT data were evaluated using BRASS brain analysis software (Hermes Medical Solutions, Stockholm, Sweden) [18]. BRASS spatially registers reconstructed tomographic data to a template and finds the count concentration in pre-defined striatal and background volumes of interest (VOI). A specially prepared template and volume of interest set was used to match the particular shape of the striatal phantom, which differs in some small details from the normal human anatomy. The sizes of the striatum and background VOIs are approximately 13.7 ml and 48.0 ml, respectively. Using the count concentrations in the volumes of interest, BRASS calculates the reconstructed striatal uptake ratios ( $SUR_{recon}$ ). SURs were calculated for both Gauss MC and Full MC and compared to the known true ratios.

## Patient data

The scans of 24 patients (mean age 56.6 years; age range 21–79 years), who were referred for clinical DaTScan study and who's studies were subsequently reported as normal, were further used to compare the two reconstruction algorithms. The subjects were scanned with the same camera

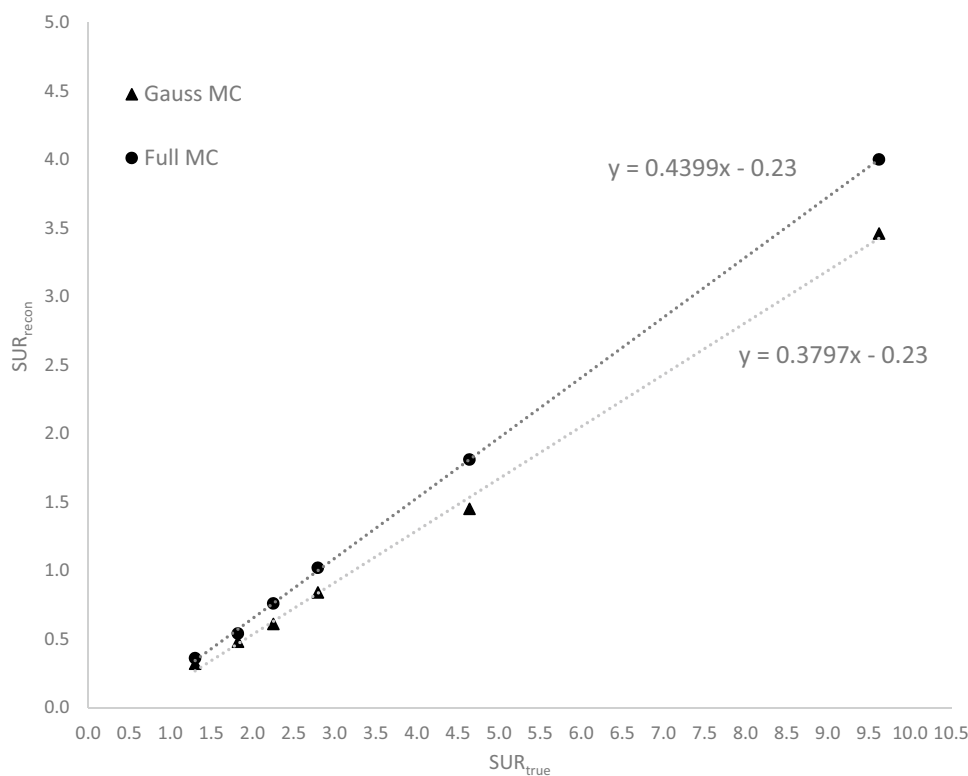
and acquisition protocol as for the phantom study described above, with the exception of the CT scan. A CT scan was not available with the patient studies because in the clinical protocol SURs are compared to a reference database, which was gathered without CT scans. The administered I-123 activity was 185 MBq and the scan was performed 3 h after the injection. The ethics committee of Päijät-Häme Central Hospital approved the use of the patient data.

Patient SPECT data were reconstructed using the same parameters as the phantom scans except for the method of attenuation correction. Attenuation correction was performed using a uniform attenuation map generated by fitting ellipses to head outline. Reconstructed SPECT data were also evaluated with the BRASS program, but using a reference template derived from the EARL normal human studies data set (EANM Research Lt). SUR values were calculated for right and left caudate (7.0 ml) and putamen (6.3 ml), for both Gauss MC and Full MC reconstructions. Background VOI was placed on the occipital cortex (approximately 32–64 ml depending on the size of the brain).

## Results

The graph in Fig. 1 plots the reconstructed SURs versus the true SURs for both reconstruction methods. Figure 1 also shows linear fits ( $SUR_{recon} = \alpha \times SUR_{true} + \beta$ ) to both plots. The equation for Gauss MC is  $0.3797x - 0.23$ , and

**Fig. 1** Reconstructed SURs as a function of true SURs. The figure also shows linear fits ( $SUR_{recon} = \alpha \times SUR_{true} + \beta$ ) to the data



$0.4399x-0.23$  for Full MC. The true and reconstructed uptake ratios are highly correlated for both reconstruction methods ( $r^2=0.9983$  for Gauss MC and  $r^2=0.9998$  for Full MC), but as can be seen from the equations the slopes ( $\alpha$ ) are well below 1. This means that the SPECT SUR underestimates the true SUR for both reconstructions, however the Full MC reconstruction does improve the SUR estimate when compared to the Gauss MC reconstruction.

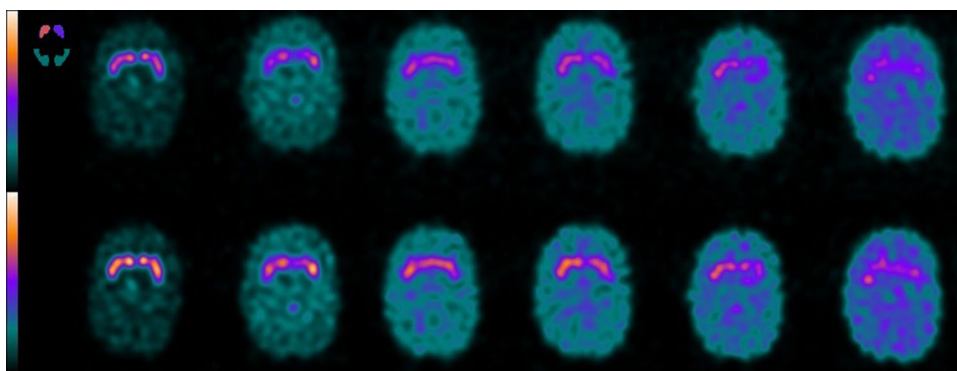
Figure 2 shows the same example slice of the I-123 phantom with the six different background concentrations for both reconstruction algorithms. A global colormap was used in the figure to demonstrate the increased recovery of

striatum uptake with Full MC algorithm compared to Gauss MC algorithm. It is evident in the figure that as the SUR value decreases the shape of the striatum is harder to discern. The striatum to background contrast appears better in the Full MC compared to Gauss MC.

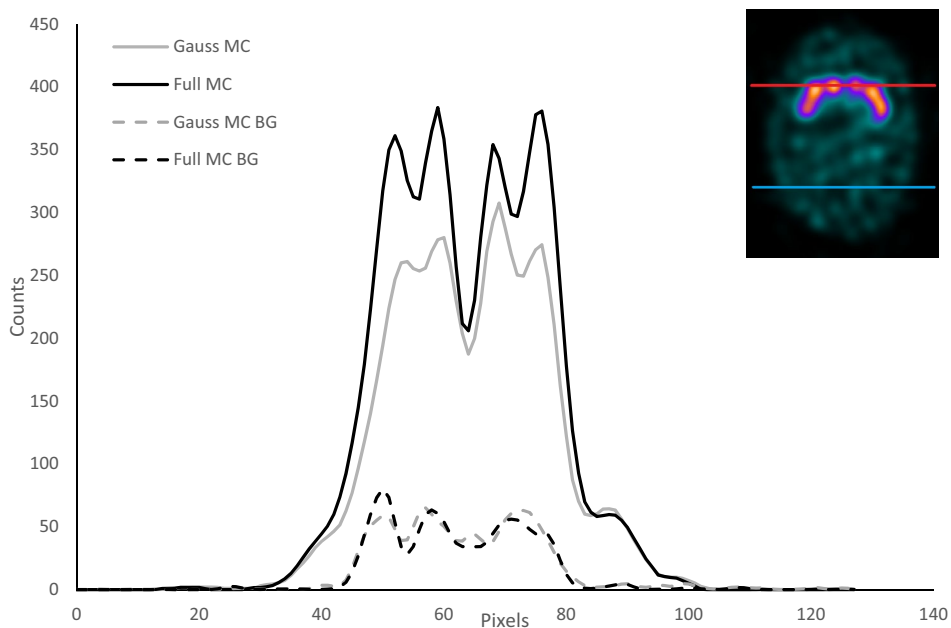
Figure 3 presents horizontal profiles that were taken through the caudate and background for both algorithms. The dataset with the highest SUR was chosen due to clarity. Full MC profiles show higher peaks and deeper valleys indicating better resolution and contrast.

Table 1 shows the mean and standard deviation (SD) of the SUR values for the patient data for both reconstruction

**Fig. 2** Example slices of the I-123 phantom with the six different SURs for Gauss MC (upper row) and Full MC (lower row) algorithms. From left to right the slices are showing SURs of 9.6, 4.6, 2.8, 2.3, 1.8 and 1.3, respectively. The small image on the top left corner shows the striatum and background VOIs



**Fig. 3** Horizontal profiles of the caudate and background for reconstructed data with SUR value of 9.6. The picture in the upper right corner shows the locations that the profiles were taken for caudate (red line) and background (blue line)



**Table 1** Mean and standard deviation (SD) of the SUR values for the patient data for the two algorithms

	SUR Gauss MC				SUR Full MC			
	Right caud	Left caud	Right put	Left put	Right caud	Left caud	Right put	Left put
Mean	3.06	3.08	2.88	2.92	3.52	3.51	3.24	3.37
SD	0.36	0.38	0.39	0.39	0.39	0.39	0.41	0.41

algorithms. Full MC yields higher mean ratios for all the striatal regions than Gauss MC, while the SD is roughly the same for both methods. In Fig. 4 the same example slices of a patient study are presented for both reconstruction algorithms. A global colormap was used in the figure to demonstrate the increased recovery of striatum uptake with Full MC algorithm compared to Gauss MC algorithm. Similarly to Fig. 2, in Fig. 4 the striatum to background contrast appears better in the Full MC compared to Gauss MC.

Horizontal profiles that were taken through the caudate and background for both algorithms are shown in Fig. 5. The dataset of the same patient study that was used in Fig. 4 was chosen for the profiles. Similarly to the phantom profiles, Full MC profiles show higher peaks and deeper valleys than Gauss MC profiles.

## Discussion

Currently I-123 reconstruction is commercially available only with geometric modeling of the CDR. This paper presents the validation of the first full CDR compensation algorithm for I-123 in a third-party commercial reconstruction software package. Full MC model was noticed to improve quantitative accuracy. Figure 1 shows a significant increase especially with higher values of SUR, when MC-based full CDR is applied in the reconstruction compared to reconstructions where only the geometric component of the CDR is compensated. With low SUR values

the differences between the two reconstruction methods diminish as the striatum uptake becomes closer to the background activity, which can also be seen in Fig. 2. Both the visual (Figs. 2, 4) and profile comparisons (Figs. 3, 5) show that the Full MC images have higher contrast and resolution therefore improving the quantitative accuracy. The SUR mean values for patient data analysis (Table 1) agree with the findings of the phantom results. Compensation for collimator scatter and septal penetration increases SURs for both phantom and patient settings.

The increase in SURs with Full MC model is due to both higher striatum counts and lower background counts (Figs. 3, 5). The improved collimator and detector model leads to better activity recovery seen mainly as increased counts in the small striatum area and reduction of the high-energy photon down-scatter contribution, which is seen as lower background in the Full MC images.

Reconstruction time has probably been the main limiting factor in the acceptance of Monte Carlo-based compensation methods. Monte Carlo-based scatter compensation methods are considered computationally demanding compared to, for example, multiple energy window subtraction methods. The average reconstruction times for Gauss MC and Full MC, respectively, were 1.4 min and 12 min (CPU: Intel Core i7-4702MQ @ 2.20 GHz). It is, however, noteworthy that in this work the reconstructions were performed without the benefit of GPU acceleration, which has been shown to be 24 times faster than CPU reconstruction [19].

**Fig. 4** Example slices of a patient study for Gauss MC (upper row) and Full MC (lower row) algorithms. The small image on the top left corner shows the striatum and background VOIs

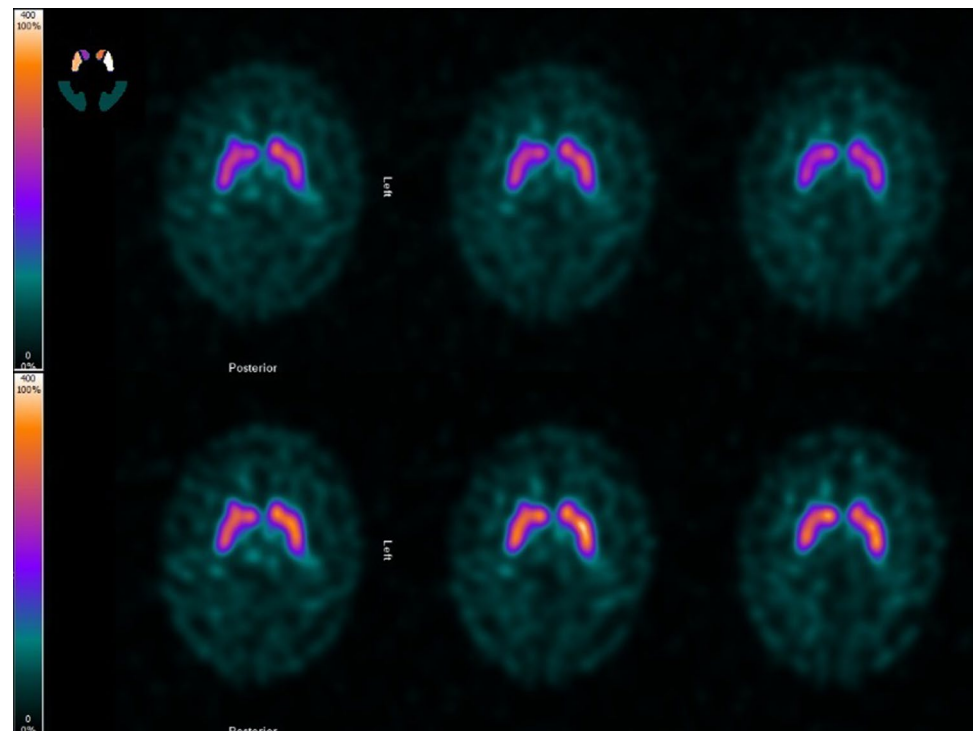
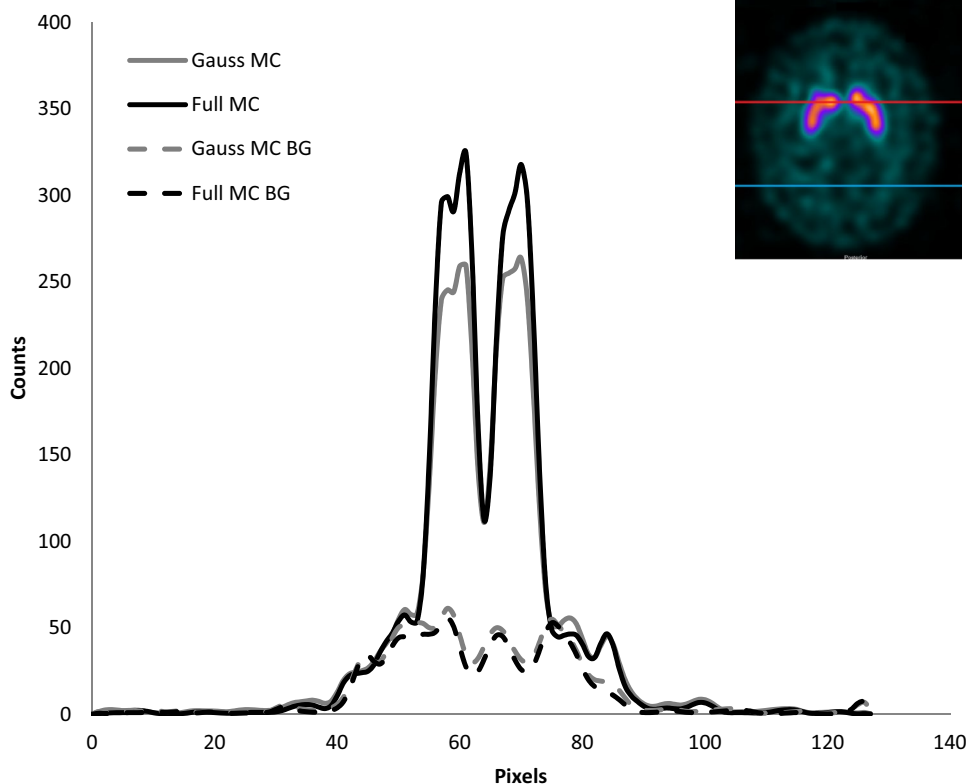


**Fig. 5** Horizontal profiles of the caudate and background for a patient study. The picture in the upper right corner shows the locations that the profiles were taken for caudate (red line) and background (blue line)



There are some limitations in this study considering the striatal phantom and the acquisition setup. Although much used in dopamine active transporter (DAT) imaging studies, the striatal phantom only extends to the base of the skull and only has activity in the brain area. Therefore, it does not take into consideration the activity or matter outside the brain which is always present in patient imaging. Therefore, the phantom studies cannot represent completely a real-world patient study in terms of the scatter and septal penetration, and the effect of that added scatter material becomes significant when using quantification with a reference database [20]. Also in this study a homogenous tracer concentration throughout the whole striatum was chosen, which is not often the case in a clinical practice. Even though the patient scan results do confirm the findings of the phantoms scans, in future it would be interesting to have more complex phantom setups for comparison, as well as a multi-center study with different manufactures' scanners.

The findings considering the Full MC compensation are in agreement with previous studies [5, 20]. Du et.al [5] showed that the down-scatter of the high energies of I-123 into the main energy window has a significant impact on the SUR and thus a full CDR compensation method is required in order to achieve good quantitative accuracy. Crespo et.al [21] demonstrated the effect of different compensation methods on quantitative accuracy in I-123 studies. They showed that PVE is

significant in DAT quantitation as the volume of the striatum is small.

CDR compensation itself reduces error due to PVE and we did not apply any specialized PVE compensation methods. Thomas et al. [22] presented in their extensive study a toolbox with various PVE compensation methods for PET imaging. In their study it was shown that PVE compensation is very sensitive to PSF mismatch and therefore requires a realistic estimate of PSF in order to work. They also showed that anatomy-based compensation algorithms performed better compared to convolution-based methods. It is evident that PVE compensation would lead to higher SURs in DAT-imaging. But utilizing a post-reconstruction PVE compensation method on low SUR images, for example the 2.3, 1.8 or 1.3  $SUR_{true}$  data in Fig. 2, could be cumbersome, because a lot of the contrast is already lost in the reconstruction process. Alternatively, PVE compensation during reconstruction using anatomical prior information with MRI might be a better choice and would be a very interesting topic for further research.

## Conclusion

The results for the use of Full MC CDR in DAT-imaging are promising if not ideal. It clearly improves the quantitative performance and visual quality of the images for both phantom and patient data, but PVE errors persist.

## References

- Eerola J, Tienari PJ, Kaakkola S, Nikkinen P, Launes J. How useful is [123I]beta-CIT SPECT in clinical practice? *J Neurol Neurosurg Psychiatry*. 2005;76:1211–6.
- Kish SJ, Shannak K, Hornykiewicz O. Uneven pattern of dopamine loss in the striatum of patients with idiopathic Parkinson's disease: pathophysiologic and clinical implications. *N Engl J Med*. 1988;318:876–80.
- Jaber M, Jones S, Giros B, Caron MG. The dopamine transporter: a crucial component regulating dopamine transmission. *Mov Disord*. 1997;12:629–33.
- Djang DSW, Janssen MJR, Bohnen N, Booij J, Henderson TA, Herholz K, et al. SNM practice guideline for dopamine transporter imaging with 123I-ioflupane SPECT 1.0. *J Nucl Med*. 2012;53:154–63.
- Darcourt J, Booij J, Tatsch K, Varrone A, Vander Borght T, Kapucu OL, et al. EANM procedure guidelines for brain neurotransmission SPECT using (123) I-labelled dopamine transporter ligands, version 2. *Eur J Nucl Med Mol Imaging*. 2010;37(2):443–50.
- Du Y, Tsui BMW, Frey EC. Model-based compensation for quantitative 123I brain SPECT imaging. *Phys Med Biol*. 2006;51:1269–82.
- Pareto D, Cot A, Pavía J, Falcón C, Juvells I, Lomeña F, et al. Iterative reconstruction with correction of the spatially variant fanbeam collimator response in neurotransmission SPET imaging. *Eur J Nucl Med Mol Imaging*. 2003;30:1322–9.
- Soret M, Koulibaly PM, Darcourt J, Hapdey S, Buvat I. Quantitative accuracy of dopaminergic neurotransmission imaging with 123I SPECT. *J Nucl Med*. 2003;44:1184–93.
- Catafau AM. Brain SPECT of dopaminergic neurotransmission: a new tool with proved clinical impact. *Nucl Med Commun*. 2001;22:1059–60.
- Hutton BF, Buvat I, Beekman FJ. Review and current status of SPECT scatter correction. *Phys Med Biol*. 2011;56:R85–R112.
- Bailey DL, Willows KP. An evidence-based review of quantitative spect imaging and potential clinical applications. *J Nucl Med*. 2013;54:83–9.
- Sohlberg A, Watabe H, Iida H. Acceleration of Monte Carlo-based scatter compensation for cardiac SPECT. *Phys Med Biol*. 2008;21:N277–285.
- Hudson M, Larkin RS. Accelerated image reconstruction using ordered subsets of projection data. *IEEE Trans Med Imaging*. 1994;13:601–9.
- Di Bella EVR, Barclay AB, Eisner RL, Schafer RW. A comparison of rotation-based methods for iterative reconstruction algorithms. *IEEE Trans Nucl Sci*. 1996;43(6):3370–6.
- de Jong H, Slijpen E, Beekman F. Acceleration of Monte Carlo SPECT simulation using convolution based forced detection. *IEEE Trans Nucl Sci*. 2001;48:58–64.
- Sohlberg A, Kajaste M. Fast Monte Carlo-simulator with full collimator and detector response modelling for SPECT. *Ann Nucl Med*. 2012;26:92–8.
- Kangasmaa TS, Constable C, Sohlberg AO. Evaluation of quantitative 123I and 131I SPECT with Monte Carlo-based down-scatter compensation. *Nucl Med Commun*. 2018;39:1097–102.
- Koch W, Radau PE, Hamann C, Tatsch K. Clinical testing of an optimized software solution for an automated, observer independent evaluation of dopamine transporter SPECT studies. *J Nucl Med*. 2005;46:1109–18.
- Bexelius T, Sohlberg A. Implementation of GPU accelerated SPECT reconstruction with Monte Carlo-based scatter correction. *Ann Nucl Med*. 2018;32:337–47.
- Tossici-Bolt L, Dickson JC, Sera T, Booij J, Asenbaun-Nan S, Bagnara MC, et al. [123I]FP-CIT ENC-DAT normal database: the impact of the reconstruction and quantification methods. *EJNMMI Physics*. 2017;4:8.
- Crespo C, Gallego J, Cot A, Falcón C, Bullich S, Pareto D, et al. Quantification of dopaminergic neurotransmission SPECT studies with 123I-labelled radioligands. A comparison between different imaging systems and data acquisition protocols using Monte Carlo simulation. *Eur J Nucl Med Mol Imaging*. 2008;35:1334–422.
- Thomas BA, Cuplov V, Bousse A, Mendes A, Thielemans K, Hutton BF, et al. PETPVC: a toolbox for performing partial volume correction techniques in positron emission tomography. *Phys Med Biol*. 2016;61:7975–93.

**Publisher's Note** Springer Nature remains neutral with regard to jurisdictional claims in published maps and institutional affiliations.